EFFICIENT ENERGETIC UTILIZATION OF GLYCEROL– STEADY STATE MODELING OF HYBRID SOLID OXIDE FUEL CELL (SOFC) AND GAS TURBINE (GT) SYSTEM*

Aline Lima da Silva[1]

Abstract
Hybrid solid oxide fuel cell/gas turbine systems (SOFC-GT) are promising innovative technology with the potential to boost distributed energy generation, due to high electrical efficiencies achieved, while keeping much lower environmental impact. In this context, the present study provides a steady-state model for a SOFC-GT architecture based on anode gas recirculation concept, with glycerol being used as a fuel. The developed code allows calculating heat and mass balance using system analysis by modeling each module, namely, reformer, SOFC stack, afterburner, heat exchanger, anode gas recirculation blower, turbine and air compressor. Adiabatic reformer was modeled according to entropy maximization technique, allowing a more straightforward integration with SOFC anode, ensuring a faster code execution. The whole process flowsheet diagram (PFD) is provided for a designed 200kW AC SOFC-GT system, yielding 66.6% electrical efficiency. Such a high efficiency is achieved for pressurized system (8 atm), SOFC stack composed of 500 cells, at a power density of 0.75 W cm^{-2} and single cell voltage of 0.842V. Enhanced electrochemical performance is obtained with the utilization of a new generation of metal-supported SOFC, based on optimized materials LSCM/YSZ/SDCN (lanthanum strontium manganite/yttria stabilized zirconia/samaria-doped ceria mixed with Ni). In addition, two-stage compression and expansion, with proper selection of rotor diameter sizes besides a fully electric technology, could result in compressors and turbines efficiencies of approximately 83% and 85%, respectively.
Keywords: Solid oxide fuel cell; Efficiency; Biofuel; Thermodynamics

[1] *PhD, Professor, Metallurgical and Materials Engineering, Federal University of Minas Gerais, Belo Horizonte, Minas Gerais, Brazil.*

1 INTRODUCTION

Since January 1st 2008, Brazil included biodiesel into its energy matrix [1]. Biodiesel has similar properties to that of diesel produced from crude oil and can be used directly to run existing diesel engines or as a mixture with crude oil diesel. The main advantages of using biodiesel is that it is biodegradable, it can be used without modifying existing engines, and produces less harmful gas emissions such as sulfur oxides [2]. Transesterification of oils is the chemical route for production ofbiodiesel,yielding glycerol as a by-product. The increasing demand for biodiesel leads to substantial production of glycerol [3].However, only a small amount of glycerol from biodiesel production is purified for use in food, pharmaceutical, tobacco and cosmetic industries. As a consequence, a glut of glycerol could be expected on the national/world market.It has been suggested that efficient and effective uses for glycerol could play an essential role in the cost reduction of biodiesel production [4].
Glycerol is a green chemical (non-toxic, non-volatile and non-flammable), which makes it ideal for a wide variety of power use [5]. In this context, chemical energy of glycerol could be efficiently converted into electricity by means of the use of solid oxide fuel cells (SOFCs).
SOFCs operate at high temperature and achieve high power generation efficiency without requiring expensive catalysts, such as platinum [6]. Due to elevated operating temperatures, SOFCs are fuel flexible and can be combined with conventional gas turbine power plants (hybrid systems). Previous analysis show that hybridization of existing fuel cell and gas turbine technologies canyieldultrahigh electrical efficiencies, in the range of65-75% [7-9]. These SOFC features are suited for distributed generation application, which can lead to widespread utilization of glycerol for electricity generation purposes.
In this work, a hybrid solid oxide fuel cell and gas turbine power system model is developed. Firstly, a sensitivity analysis is carried out, where the effect of system operating pressure and anode fuel utilization on overall system performance is evaluated. In this preliminary part, turbine, compressor and anode recycle blower efficiencies are only estimated and included as constant values in the model. Then, the most appropriate operating conditions, focusing on system efficiency and minimum number of cells, are suggested. Finally, a whole analysis at the selected design pointis presented for a SOFC-GT system of 200kW, including the process flowsheet diagram (PFD). In this analysis, more realistic models for compressor, blower and turbine are considered. Detailed performance maps are presented, and a methodology for selecting suitable rotor sizes is adopted. Staged compression and expansion are simulated for achieving high efficiencies values, and,at each stage, it is assumed that the compressor is connected to the expander via an electrical link between the motor and generator, allowing the compressor and expander shafts to operate at different velocities [8]. In addition, it is worth pointing out that SOFC electrochemicalmodel is built based on polarization performance of high power density metal-supported SOFCs (MS-SOFCs).New generation of MS-SOFCs display a number of advantages over conventional all-ceramic SOFCs, including low-cost structural materials, mechanical ruggedness, excellent tolerance to redox cycling, and extremally fast start-up capability [10].
It is also worth mentioning that 200 kW SOFC has been recently selected as commercialization platform by fuel cells developers, such as Fuel Cell Energy, Inc. and Mitsubishi Hitachi Power Systems, Ltd. In this sense, the power size of the proposed hybrid architecture is in accordance with the main global trends.

2 METHODOLOGY

2.1 SOFC-GT hybrid power system operating with glycerol

Figure 1 shows the proposed architecture for the SOFC-GT hybrid power system. Each material stream was identified with a number, from #1 to #13, to facilitate the description of the system. Glycerol (#1) is converted into smaller molecules (H_2, CO, CO_2, CH_4) by reaction with steam and CO_2 in an adiabatic reformer. The anode outlet gas itself (#4) is used in the reforming process. This approach has the advantage of utilization of high temperature (800 °C)anode exhaustgas, which is rich in CO_2 and H_2O; thus, all steam for glycerol conversion as well asthe sensible heat for heating and evaporating liquid glycerol (#1) besides sustaining endothermic reactions in the reformer comes from the anode exhaust gas.The amount of gas from the anode to be routed to the reformer (#5) should be selected in such a way that the resulting steam-to-carbon ratio (S/C ratio) in the reformer inlet mixture results in carbon deposition free conditions from a thermodynamic viewpoint. The remaining part of the anode outlet gas is routed to the combustor (#6).The gas leaving the reformer (#2) passes through the anode recirculation blower, where small pressure losses are compensated, and it enters into the anode (#3), where chemical reactions (methane internal reforming, water-gas shift) and the electrochemical reaction of hydrogen oxidation occur.The air introduced into the cathode (#9) is initially compressed (#7) and then passes through a heat exchanger, HX (#8), which ensures a suitable inlet temperature into the cell; it is recommended that the temperature variation between the inlet and the outlet gases at the anode and cathode being at most 200 °C. The heating of the incoming air occurs by the use of thermal energy of the cathode output gases (#10).In order to keep the SOFC temperature constant, the cathode must be operated with excess air so that the heat balance in the stack is satisfied. The residual oxygen in the cathode output gas (#11) is used in the combustion reaction, where it reacts with the residual species present in the anode outlet gas (H_2, CH_4, CO) (#6).Finally, the combustor outlet gas (#12) is directed to the turbine where it is expanded, and the exhaust gas (#13) is released.

2.2. Mass and energy balance of the system

The steady-state model was implemented in Visual Basic. The algorithm flowchart is depicted in **Figure 2**. Basically, it consists of the following steps: (1) definition of operating parameters,(2) estimation of the flow rate and composition of the anode exhaust gas, as well the estimation of air excess ratio; (3) iterative resolution of the reformer and fuel cell models, in order to ensure that the reformer is adiabatic and the thermal balance applied to the SOFC stack is satisfied; (4) sequential resolution of air compressors, heat exchanger, afterburner, turbine models; (5) calculation of DC and AC system efficiencies. For a given set of operational parameters, the algorithm provides the whole process flowsheet diagram (PFD), that is, the composition, temperature and pressure for each material stream identified in the SOFC-GT system. In order to solve the several models described in the algorithm flowchart, an optimization algorithm was employed. In the next section, a brief description of the component models is provided.

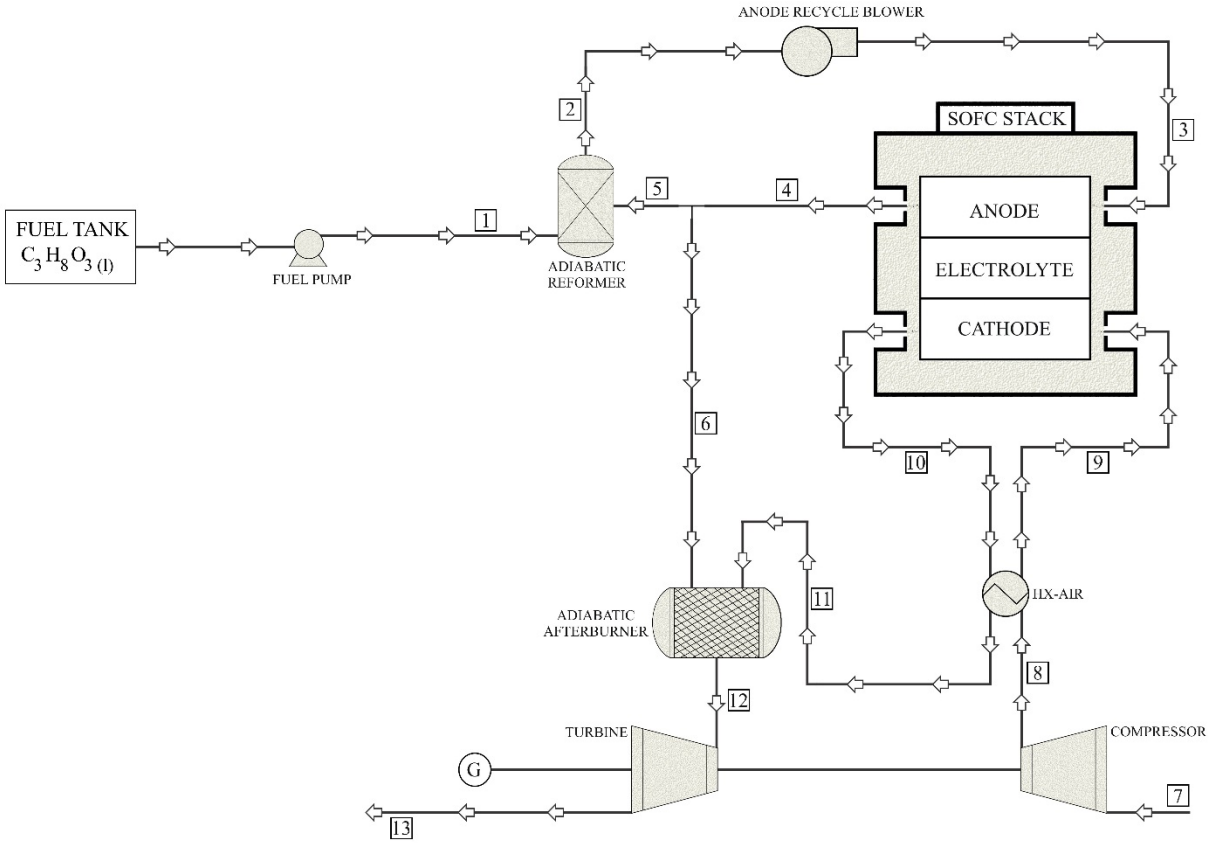

Figure 1. SOFC-GT hybrid power system architecture

2.3. Models Development

2.3.1. Adiabatic Reformer

The equilibrium composition and temperature of reformer outlet gas were simultaneously determined through the entropy maximization technique. The optimization method seeks the maximum value for the system entropy (objective function, Eq. (1)) constrained by the elemental mass balance (Eq. (2)) and by isenthalpic condition (Eq. (3)) (restrictions).

$$S_{system} = \sum \dot{n}_i \bar{S}_i^0 - R \sum \dot{n}_i \ln(x_i P_{system}) \quad (1)$$

$$\sum_{i=1}^{N} \dot{n}_i \alpha_{ik} = b_k \quad (2)$$

$$\sum \dot{n}_{i,in} (\bar{H}_i)_{T=T_{inlet\_reformer}} - \sum \dot{n}_{i,out} (\bar{H}_i)_{T=T_{outlet\_reformer}} - \Delta H_{C_3H_8O_{3(L)} \rightarrow C_3H_8O_{3(G)}} = 0 \quad (3)$$

where

$$\Delta H_{C_3H_8O_{3(L)} \rightarrow C_3H_8O_{3(G)}} = \dot{n}_{C_3H_8O_3} \left[\bar{C}_{P(L)} (T_{evaporation} - 298) + \Delta \bar{H}_{evaporation} \right] \quad (4)$$

In Eqs. (3)-(4), n_i and x_i correspond to molar flowrate (moles·s^{-1}) and molar fraction of species i, respectively; b_k is the number of moles of component k (C, H, O) in the system, and α_{ik} is the number of moles of component k in species i. In this study, $i \in \{C_3H_8O_3, H_2, H_2O, CH_4, CO, CO_2, C_{graphite}\}$.

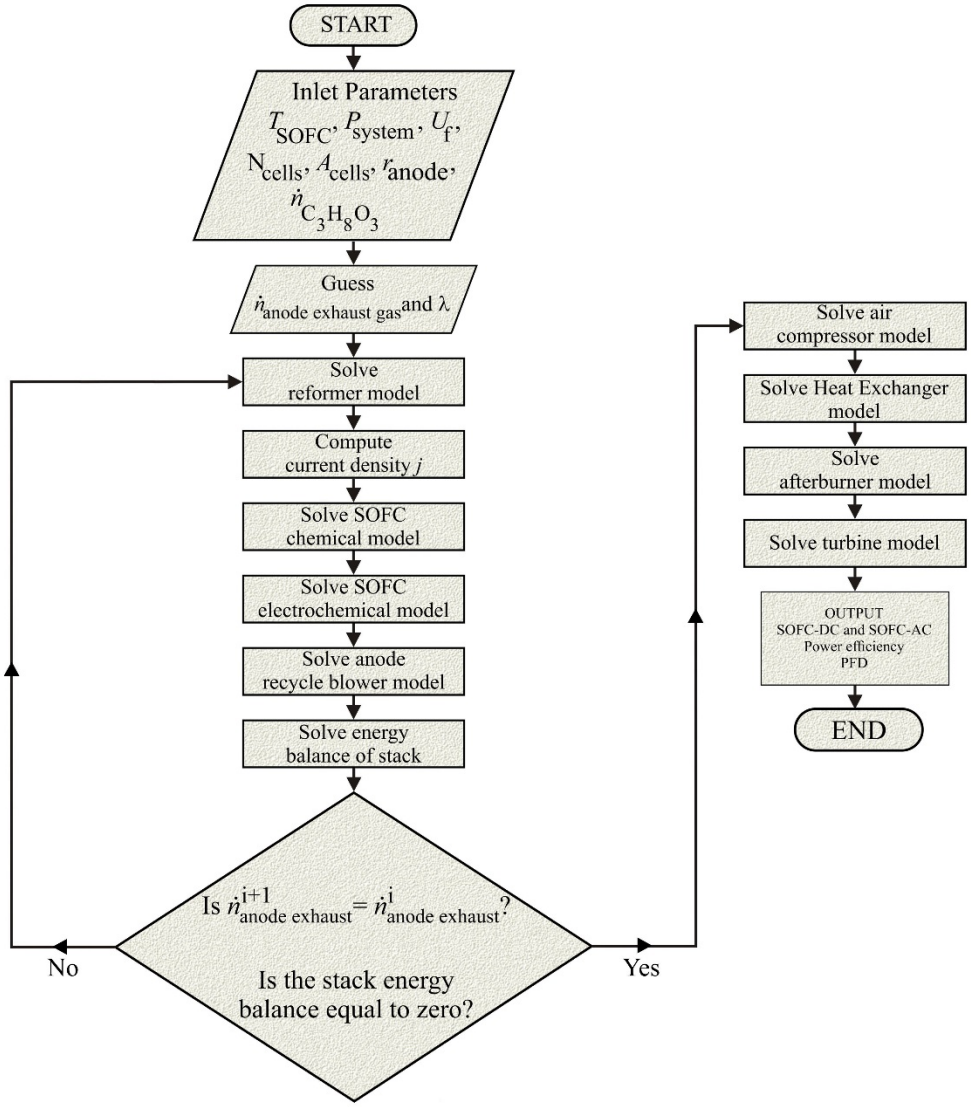

Figure 2. Solution algorithm of the SOFC-GT hybrid power system model

2.3.2. Solid Oxide Fuel Cell

2.3.2.1. Electrochemical Model

The SOFC operating potential (*U*) for a given current density *j* is:

$$U = U_{OCV} - jR_{ohm} - \frac{2RT}{ZF} sinh^{-1}\left(\frac{j}{2j_{0,a}}\right) - \frac{2RT}{ZF} sinh^{-1}\left(\frac{j}{2j_{0,c}}\right) + \frac{RT}{ZF} ln\left(1 - \frac{j}{j_L}\right) \quad (5)$$

where U_{OCV} is the reversible open circuit voltage given by the Nernst equation.The exchange current density at anode and cathode are calculated as follows:

$$j_{0,anode} = \gamma_{anode} \left(\frac{x_{H_2} P_a}{P^0}\right)\left(\frac{x_{H_2O} P_a}{P^0}\right) exp\left(\frac{E_{anode}}{RT}\right) \quad (6)$$

$$j_{0,cathode} = \gamma_{cathode} \left(\frac{x_{O_2} P_{cathode}}{P^0}\right)^{0.25} exp\left(\frac{E_{cathode}}{RT}\right) \quad (7)$$

where γ_{anode} and $\gamma_{cathode}$ are exchange current density constants, and E_{anode} and $E_{cathode}$ are activation energy at the anode and cathode, respectively. A least-square

non-linear regression method is employed to calibrate γ_{anode}, $\gamma_{cathode}$, E_{anode} and $E_{cathode}$. The model has been calibrated against a polarization curve published by Tucker [10], for very highpower density LSM/YSZ/SDCN(lanthanum strontium manganite/yttria stabilized zirconia/samaria-doped ceria mixed with Ni) metal-supported SOFCs. The comparison between model and experimental data can be seen in **Figure 3**.

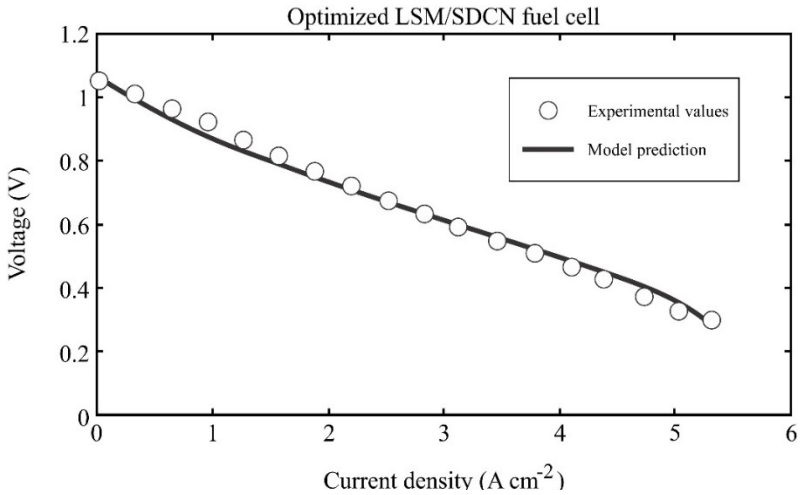

Figure 3. Experimental data from polarization curve obtained for LSM/YSZ/SDCN metal-supported fuel cell, reported by Tucker [10], along with theoretical curve predicted by the model developed in the present study.

2.3.2.2. Chemical Model

For determination of the molar composition of the anode and cathode exhaust gas, the kinetics of three reactions occurring at the anode (methane internal reforming R1, water-gas shift R2, and hydrogen electrochemical oxidation R3), and the electrochemical reduction reaction at the cathode, R4, are considered:

$$CH_4 + H_2O \leftrightarrow CO + 3H_2 \quad \text{(R1)}$$

$$CO + H_2O \leftrightarrow CO_2 + H_2 \quad \text{(R2)}$$

$$H_2 + O^{2-} \leftrightarrow H_2O + 2e^- \quad \text{(R3)}$$

$$(1/2)\ O_2 + 2e^- \leftrightarrow O^{2-} \quad \text{(R4)}$$

Then, the system of equations to determine the number of moles of each species $i(n_i)$ at the anode exhaust is given by:

$$n_i = n_i^0 + A_{cell} \sum \upsilon_{i\phi}\, r_\phi \quad (8)$$

where $\upsilon_{i\phi}$ is the stoichiometric coefficient of the species *i* in the reaction ϕ. The reaction rates (r_ϕ) for the above reactions are given by:

$$r_{R1=} k_{R1} P_a x_{CH_4} exp\left(\frac{-E_A}{RT}\right) \quad (9)$$

$$r_{R2} = k_{R2} P_a x_{CO} \left(1 - \frac{x_{CO_2} x_{H_2} / x_{CO} x_{H_2O}}{K_{R2}}\right) \quad (10)$$

$$r_{R3} = r_{R4} = \frac{j}{2F} \quad (11)$$

2.3.2.3. Energy balance of SOFC stack

The energy balance of the stack is defined as follows [11]:

$$\sum \dot{n}_{i,in} (\bar{H}_i)_{T=T_{inlet}} = \sum \dot{n}_{i,out} (\bar{H}_i)_{T=T_{outlet}} + P_{SOFC-DC} \quad (12)$$

where $P_{SOFC-DC}$ is DC power produced by SOFC stack, and it is given by:

$$P_{SOFC-DC} = N_{cells} A_{cell} jU \quad (13)$$

To keep the SOFC stack at a constant temperature, some cooling of the stack is required. Some cooling is achieved by endothermic reforming of methane; besides, fuel is not at the SOFC operating temperature when it enters the anode (generally, $T_{fuel} < T_{SOFC}$), which also provides a cooling effect. However, additional cooling is still required, and stack temperature can be kept constant when excess air is supplied to the cathode. The excess air ratio (λ)is defined as the ratio between the moles of oxygen supplied with air and moles of oxygen needed for electrochemical reaction. Thus, by solving Eq. (12), excess air ratio is determined.

2.3.3. Compressor, anode recycle blower and turbine

2.3.3.1. Compressor and blower thermodynamic model

Based on perfect gas equations and polytropic transformations [12], the exhaust temperature can be determined by the following equation:

$$T_e = T_i \left(\frac{p_e}{p_i}\right)^{\frac{(\gamma-1)}{\gamma \eta_p}} \quad (14)$$

Where $\gamma = {C_P}/{C_V}$, and η_P is polytropic efficiency of the compressor.

Change in isentropic enthalpy is given by:

$$\Delta h_C = C_P T_i \left[\left(\frac{p_e}{p_i}\right)^{\frac{(\gamma-1)}{\gamma \eta_p}} - 1\right] \quad (15)$$

The compressor efficiency (η_C) is calculated by the following relationship:

$$\eta_C = \frac{\left(\frac{p_e}{p_i}\right)^{\frac{(\gamma-1)}{\gamma}} - 1}{\left(\frac{p_e}{p_i}\right)^{\frac{(\gamma-1)}{\gamma \eta_p}} - 1} \quad (16)$$

Compressor power consumption is calculated by:

$$P_C = \bar{C}_P \Delta T_C n_C \quad (17)$$

2.3.3.2. Turbine thermodynamic model

Turbine has been modeled in the same way as the compressor, following a polytropic expansion. The exhaust temperature:

$$T_e = T_i \left(\frac{p_e}{p_i}\right)^{\frac{(\gamma-1)\eta_p}{\gamma}} \quad (18)$$

Change in isentropic enthalpy:

$$\Delta h_T = C_P T_i \left[\left(\frac{p_e}{p_i}\right)^{\frac{(\gamma-1)\eta_p}{\gamma}} - 1\right] \quad (19)$$

Turbine efficiency (η_T):

$$\eta_T = \frac{1-\left(\frac{p_e}{p_i}\right)^{\frac{(\gamma-1)\eta_p}{\gamma}}}{1-\left(\frac{p_e}{p_i}\right)^{\frac{(\gamma-1)}{\gamma}}} \quad (20)$$

Turbine power generation is calculated by:

$$P_T = \bar{C}_P \Delta T_T n_T \quad (21)$$

2.3.3.3. Method to implement non-dimensional performance maps – scalable approach to determine suitable compressor and turbine rotor diameter sizes

In order to determine the exhaust temperature, as well as the power, one need to know the compressor and turbine efficiencies. In this way, one seeks performance maps from different manufacturers and try to identify the suitable device for the selected application. However, finding the most suitable compressor/turbine for a given application is a hard task, and the most efficient selection is not ensured. In this way, the approach developed by Bell and coworkers [13] is adopted in this study. Essentially, a dimensional analysis technique is employed to generate a suitable map once (generic, non-dimensional), and then adapt the map for use in simulation across a range of sizes. For the analysis applied to SOFC-GT system 200kW, a DLR compressor was used as baseline for scaling. Dimensional analysis was applied, in which the mass flow parameter and efficiency data supplied by manufacturer are converted into non-dimensional compressor mass flow coefficient, θ_C, and Mach numberbased on the rotor tip speed. For implementing the program, a mathematical expression of efficiency as a function of θ_C and pressure ratio is required. In this way, it was verified that a 4th order polynomial is sufficient to portray efficiency curves [14].Thus, a least-square non-linear regression method was employed.The same reasoning is valid for turbine and anode recycle blower. Turbine Capstone C30 and the anode recycle blower from R&D Dynamics were used as baseline for scaling.

Then, the user estimates the rotor diameter size before running the code. During the simulation, mass flowrate is computed and converted into non-dimensional parameter, which serves as input for the 4th order polynomial,yielding a certain efficiency value, for a selected pressure ratio.

2.3.3.4. Electronic link between compressor and turbine – estimate of power generation

It is considered that the expander and compressor are electronically rather than mechanically linked. This approach allows compressor and expander shafts to operate at different velocities. The concept relies on using a variable speed electric motor to drive a centrifugal compressor using energy supplied by a turbine-driven generator in the exhaust.Decoupling the turbine from the compressor allows the motor and generator to run at independent, optimum speed [15]. This can be done at each stage, with one compressor and one expander. In this study, two stages are considered in the design point analysis. At each stage, turbine shouldideally produce more power than that required by the compression; mechanical power is assumed to be converted into electrical AC at 76.8% efficiency (96% gearbox) ×(80%mechanical to AC)[8].It is assumed an efficiency of 95% for electric motor to drive centrifugal compressor.In case more energy is required for compression than is available from expansion, it is considered that an electrical motor provides additional power, subtracting power generated from SOFC after inverter DC/AC.

2.3.4. Heat Exchanger

By applying heat balance around air heat exchanger (HX-air) volume control, one can readily determine afterburner inlet temperature (T#11) and exchanged heat; T#8 is determined by compressor model, T#9 is fixed at 973K, T#10 is the same as the stack. At design point, an estimate of the size of a plate heat exchanger (H095 series, Kaori [16]) is provided. For this analysis, the log mean temperature approach (LMTD) has been employed (Eqs. (22)-(23)) along with empirical relationship for Nusselt number (Eq. (24)). Detailed calculation procedure can be seen elsewhere [17].

$$q = UA_s\,\Delta T_{LMTD} \quad (22)$$

$$\Delta T_{LMTD} = \frac{\Delta T_1 - \Delta T_2}{ln\left(\frac{\Delta T_1}{\Delta T_2}\right)} \quad (23)$$

$$Nu = 0.28\,Re^{0.65}\,Pr^{0.4} \quad (24)$$

2.3.5. Afterburner

The equilibrium composition and temperature of afterburner outlet gas were determined through the entropy maximization technique, in a procedure similar to that of reformer. In this case, the selected species were: $\{H_2, H_2O, CH_4, CO, CO_2, O_2, N_2, NO, NO_2, N_2O\}$.One found that the only stable species were H_2O, CO_2, O_2 and N_2. NO_x species molar fraction was always lower than 10^{-5}.

3. RESULTS AND DISCUSSION

3.1. Sensitivity analysis: effect of anode fuel utilization (U_f) and system operating pressure

From results shown in **Table 1**, one can see that for a fixed system pressure (*e.g.* 8 atm), the increase in U_f results in decrease of single cell voltage (due to higher H_2O contents in anode) and increase in SOFC DC power, due to higher power density. However, demand of air for cooling stack increases, leading to higher power consumption in compressors; at the same time, higher $U_f$diminishes inlet turbine temperature, and power generated by expansion is not enough to supply compressor demand, which diminishes overall electric efficiency, because power must be subtracted from AC power generated by SOFC after inverter. Higher $U_f$corresponds to increased amount of H_2O at anode outlet, leading to higher CH_4 conversion through endothermic reactions, resulting in lower reformer adiabatic temperatures. The highest efficiency was achieved at U_f=0.47, and power generated from expansion in turbine was enough to drive the motor coupled to the compressor. Even at a relatively low anode fuel utilization, the SOFC/GT system efficiency is greater than 66%, because the anode recirculation ratio assumed is very high (85%), which increases the overall fuel utilization of the system. These finding are in agreement with those reported by Braun et al. [18]. For sensitivity analysis, compressor and turbines efficiencies are assumed as 83.3% and 85.4 %, respectively. In design point analysis (section 3.2), compressors and turbines models are included in the code for a proper estimation of efficiencies at each stage.

Table 1. Effect of anode fuel utilizationand system operating pressure on SOFC/GT system performance. Inlet glycerol mass flowrate: 0.03604 kg·s^{-1}

System pressure [atm]	8					1.5				
Anodefuelutilization, U_f	0.47	0.57	0.67	0.77	0.87	0.47	0.57	0.67	0.77	0.87
Single cellvoltage (V)	0.842	0.831	0.819	0.808	0.798	0.842	0.831	0.819	0.808	0.798
Power density (W cm^{-2})	0.75	0.77	0.79	0.80	0.81	0.34	0.35	0.36	0.37	0.37
SOFC DC power (kW)	206.3	213.7	218.5	221.6	223.6	206.2	213.8	218.5	221.6	223.6
Numberofcells	500	500	500	500	500	1095	1110	1100	1095	1095
Anode recycle blower consumption (kW)	0.95	0.94	0.93	0.92	0.91	4.79	4.75	4.73	4.71	4.69
Air excesso ratio	1.75	2.55	3.19	3.71	4.16	2.11	2.87	3.50	4.02	4.46
Heat duty (Heat exchanger), kW	63.1	96.4	125.0	149.7	171.4	123.1	175.6	221.8	261.8	297.2
Inlet turbine temperature (K)	1039.8	888.3	818.0	778.6	753.8	806.6	668.1	598.1	557.4	531.2
Net AC power from compressor/ turbine (kW)	9.22	-2.52	-12.54	-21.05	-28.40	1.09	-1.69	-4.12	-6.19	-7.99
Net AC efficiency (%)	66.7	65.1	63.3	61.4	59.6	62.7	64.1	64.8	65.1	65.1
Reformeroutlettemperature (K)	917.3	904.9	895.0	886.9	880.3	870.8	863.8	858.7	854.7	851.7
CH_4 (%) reformergas	1.6	1.3	1.1	1.0	0.8	0.6	0.4	0.3	0.2	0.2
H_2 (%) reformergas	15.4	13.7	12.4	11.3	10.5	18.9	16.8	15.2	13.8	12.7

One can see that at the same fuel utilization and single cell voltage, the number of cells is dramatically increased,from 500 to nearly 1100, when system operating

pressure is reduced from 8 to 1.5 atm. Based on these findings, anode fuel utilization of 47%, high anode recirculation ratio (85%) and pressurized system (8 atm) were selected for designing the 200kW AC SOFC/GT system.

3.2. Hybrid SOFC/GT system operating on glycerol designed at net 200kW AC

The process flowsheet diagram (PFD) for the architecture depicted in **Figure 1** is shown in **Table 2** with each material stream given in terms of mass flowrate.**Table 3** shows thePFD given in terms of molar concentration (mol%).

Table 2. Process flowsheet diagram for hybrid SOFC/GT system running on glycerol. Mass flowrate ($kg \cdot s^{-1}$), temperature (K) and pressure (atm) is shown for each stream (#1 to #13, see**Figure 1**).

Species	#1	#2	#3	#4	#5	#6	#7	#8	#9	#10	#11	#12	#13
H_2O	0	0.06969	0.06969	0.08700	0.07395	0.01305	0	0	0	0	0	0.01526	0.01526
CH_4	0	0.00248	0.00248	0.00023	0.00020	0.00003	0	0	0	0	0	0	0
CO	0	0.01705	0.01705	0.01630	0.01386	0.00245	0	0	0	0	0	0	0
CO_2	0	0.15295	0.15295	0.16030	0.13626	0.02405	0	0	0	0	0	0.02798	0.02798
H_2	0	0.00294	0.00294	0.00158	0.00135	0.00024	0	0	0	0	0	0	0
$C_3H_8O_3$(g)	0	0	0	0	0	0	0	0	0	0	0	0	0
$C_3H_8O_3$(l)	0.03604	0	0	0	0	0	0	0	0	0	0	0	0
O_2	0	0	0	0	0	0	0.03569	0.03569	0.03569	0.01538	0.01538	0.01194	0.01194
N_2	0	0	0	0	0	0	0.11747	0.11747	0.11747	0.11747	0.11747	0.11747	0.11747
Temperature	298.0	917.3	919.4	1073.0	1073.0	1073.0	298.0	594.2	973.0	1073.0	645.9	1036.3	690.9
Pressure	8.000	7.985	8.056	8.000	8.000	8.000	1.000	8.120	8.050	8.000	7.930	7.930	0.976

Table 3. Process flowsheet diagram for hybrid SOFC/GT system running on glycerol. Molar concentration (mol%), temperature (K) and pressure (atm) is shown for each stream (#1 to #13)

Species	#1	#2	#3	#4	#5	#6	#7	#8	#9	#10	#11	#12	#13
H_2O	0	40.40	40.40	49.00	49.00	49.00	0	0	0	0	0	8.84	8.84
CH_4	0	1.62	1.62	0.15	0.15	0.15	0	0	0	0	0	0	0
CO	0	6.35	6.35	5.90	5.90	5.90	0	0	0	0	0	0	0
CO_2	0	36.27	36.27	36.93	36.93	36.93	0	0	0	0	0	16.21	16.21
H_2	0	15.36	15.36	8.02	8.02	8.02	0	0	0	0	0	0	0
$C_3H_8O_3$(g)	0	0	0	0	0	0	0	0	0	0	0	0	0
$C_3H_8O_3$(l)	100	0	0	0	0	0	0	0	0	0	0	0	0
O_2	0	0	0	0	0	0	21	21	21	11.58	11.58	6.92	6.92
N_2	0	0	0	0	0	0	79	79	79	88.42	88.42	68.04	68.04
Temperature	298.0	917.3	919.4	1073.0	1073.0	1073.0	298.0	594.2	973.0	1073.0	645.9	1036.3	690.9
Pressure	8	7.985	8.056	8	8	8	1	8.12	8.05	8	7.93	7.93	0.9763

Table 4 shows a summary of the main performance data for designed hybrid SOFC/GT system. **Figures 4 and 5**show modeled performance maps for anode recycle blower, compressors and turbines along with design point of operation.

Table 4. Inlet conditions and performance data for SOFC/GT 200kW

Inletparameters	Anoderecirculationratio (%)	85
	Numberofcells	500
	Stackoperatingtemperature (K)	1073
	System operatingpressure (atm)	8
	Single cell active area (cm^2)	552
	Inverter efficiency (%)	94
Output values	Air excesso ratio (λ)	1.76
	SOFC DC power (kW)	206.3
	Single cell (V)	0.842
	Power density (W cm^{-2})	0.75
	Number of stacks (100 cells per stack)	5
	Number of heat exchangerplates (H095 series, Kaori)	111
	First stage compressor power consumption (kW)	22.18
	First stage turbine power production (kW)	41.5
	First stage net AC power (kW)	8.53
	Second stage compressor power consumption (kW)	24.28
	Second stage turbine power production (kW)	33.98
	Second stage net AC power (kW)	0.54
	Total net AC power produced from turbine (kW)	9.07
	SOFC AC power (KW)	193.9
	Anode recycle blower power consumption (kW)	0.952
	SOFC/GT system net AC power (kW)	202.02
	Net AC electricalefficiency (%)	66.6

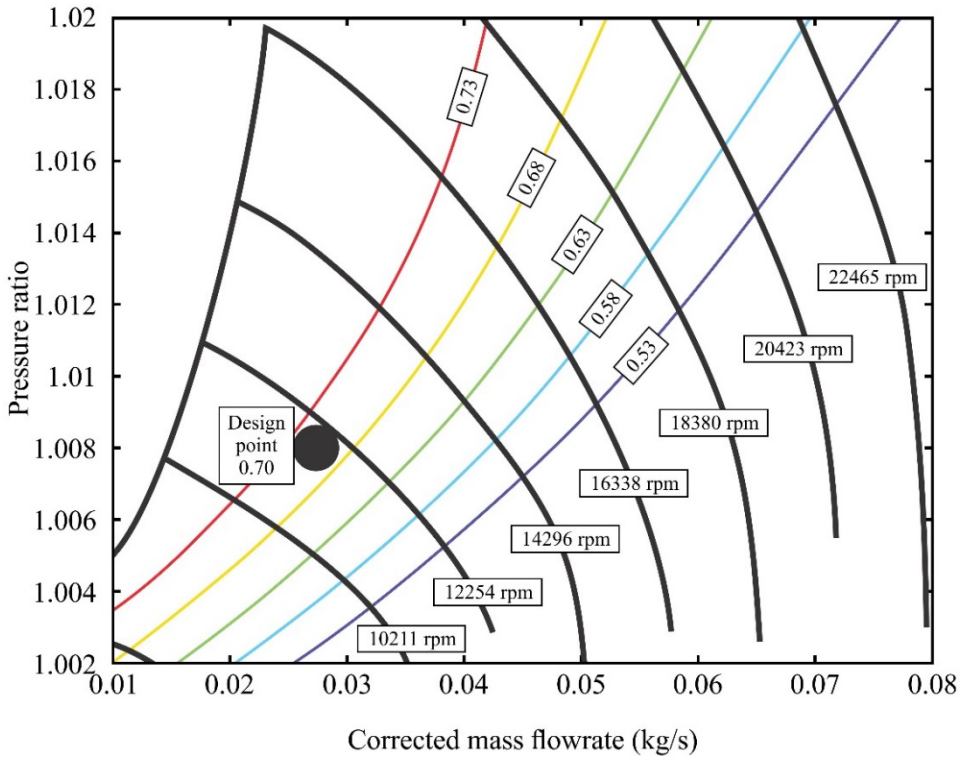

Figure 4. Modeled anode recycle blower and design operating point. R&D Dynamics original blower was scaled up to rotor diameter of 152mm. Polynomial fit with residuals lower than 10^{-3}.

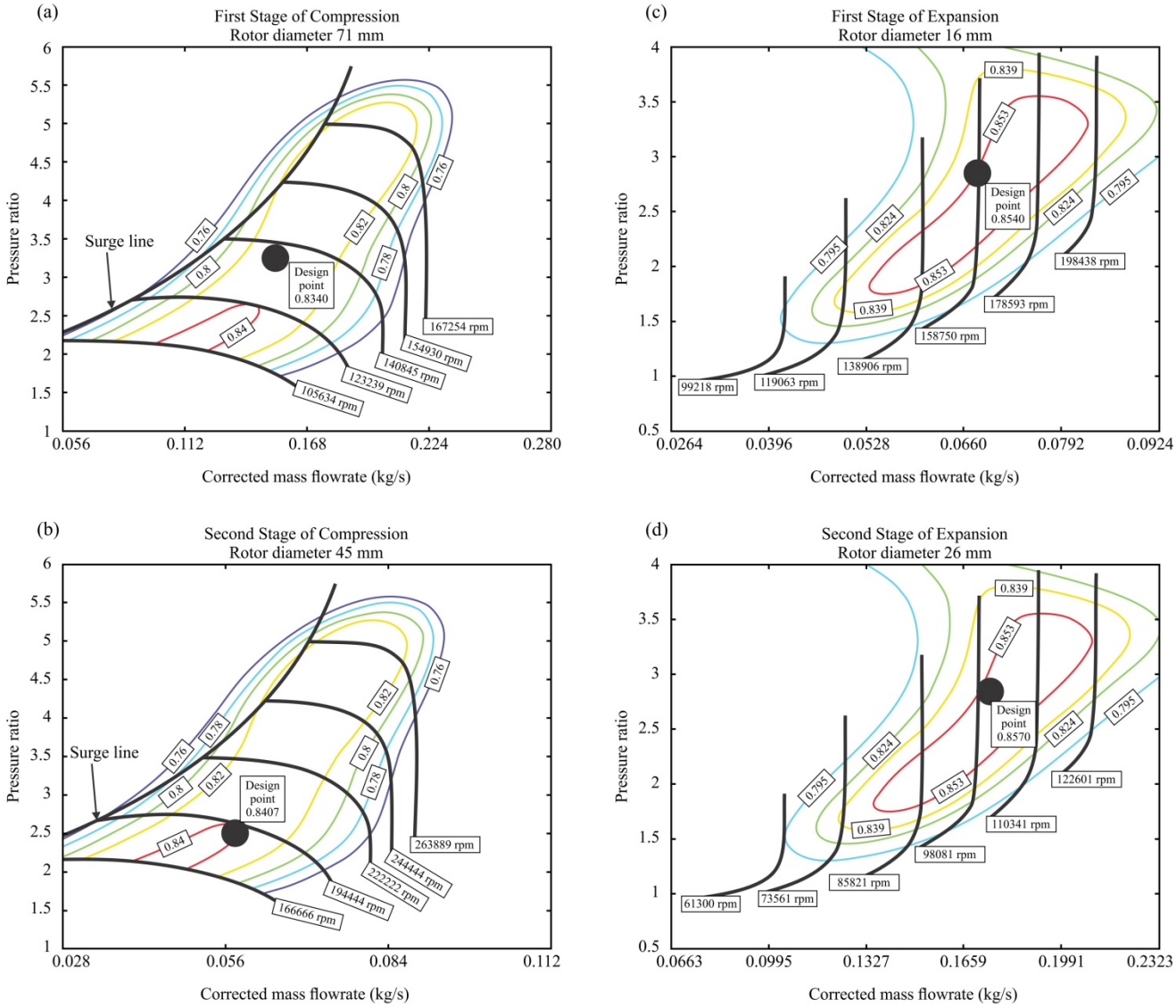

Figure 5. Modeled compressors and turbines along with design operating points. DLR compressor was scaled down to rotor diameters of (a) 71 mm (first stage of compression) and (b) 45mm (second stage of compression). Capstone turbine C30 was scaled down to rotor diameters of (c) 16mm (first stage of expansion) and (d) 26mm (second stage of expansion). Polynomial fit with residuals lower than 10^{-3}.

3CONCLUSION

A mathematical model based on thermodynamics was developed to compute process flowsheet diagram (PFD) and carry out performance analysis of a hybrid SOFC/GT system. In the present study, application was focused on glycerol; however, the code can be easily adapted for different fuels. A net 200kW AC SOFC/GT hybrid system operating on glycerol yielding 66.6% of electrical efficiency was designed from a thermodynamic viewpoint, and detailed PFD was provided. In future, it is believed that the proposed architecture can contribute to boost distributed generation from renewables, due to very high electrical efficiency and fuel versatility.With the help of developed code, it was possible to estimate number of cells in stack, electrochemical parameters of operation of SOFCs, first estimate of compressor and turbine rotor diameter sizes and stages of operation, as well as

dimensioning of anode recycle blower, besides the size of heat exchanger. Design solution based on relatively low anode fuel utilization, of nearly 50%, high anode recirculation ratio (85%) and pressurized system (8atm) is preferable for maximizing efficiency while keeping the number of cells in stack at minimum. Finally, keeping low stack fuel utilization could be beneficial for increase the lifetime of the stack.

Acknowledgments

The author would like to thank PRPq-UFMG for assistance to the research of newly appointed professors (ADRC-2016).

REFERENCES

1 Leoneti AB, Leoneti VA, Valle S, Oliveira WB.Glycerol as a by-product of biodiesel production in Brazil: alternatives for the use of unrefined glycerol. Renewable Energy. 2012; 138-145.
2 Ondul E, Dizge N. Glycerol: a major by-product in the biodiesel manufacturing process. Journal of the Institute of Natural & Applied Sciences. 2014; 19: 75-79.
3 Papanikolao S, Aggelis G. Biotechnological valorization of biodiesel derived glycerol waste through production of single cell oil and citric acid by *Yarrowialipolytica.* Lipid Technology. 2009; 21: 83-87.
4 Lima da Silva A, Muller IL.Operation of solid oxide fuel cells on glycerol fuel: a thermodynamic analysis using the Gibbs free energy minimization approach. Journal of Power Sources. 2010; 195: 5637-5644.
5 Arechederra RL, Treu BL, Minteer SD. Development of glycerol/O_2 biofuel cell. Journal of Power Sources. 2007; 173:156-61.
6 Torii R, Tachikawa Y, Sasaki K, Ito K. Anode gas recirculation for improving the performance and cost of a 5kW solid oxide fuel cell system. Journal of Power Sources. 2016;325: 229-237.
7 McLarty D, Brower J, Samuelsen S. Hybrid fuel cell gas turbine system design and optimization. Journal of Fuel Science and Technology. 2013; 041005.
8 Whyatt GA, Chick LA. Electrical Generation for More-Electric Aircraft using Solid Oxide Fuel Cells. Pacific Northwest National Laboratory, Richland, 2012.
9 Yi JH, Kim TS. Effects of fuel utilization on performance of SOFC/gas turbine combined power generation systems. Journal of mechanical Science and technology. 2017; 31: 3091-3100.
10 Tucker MA. Development of high power density metal-supported solid oxide fuel cells. Energy Technology. 2017; 5: 2175-2181.
11 Liso V, Olesen AC, Nielsen MP, Kaer SK. Performance comparison between partial oxidation and methane steam reforming processes for solid oxide fuel cell (SOFC) micro combined heat and power (CHP) system. Energy. 2011; 36: 4216-4226.
12 Chinda P, Brault P. The hybrid solid oxide fuel cell (SOFC) and gas turbine (GT) systems steady state modeling. International Journal of Hydrogen Energy. 2012; 37: 9237-9248.
13 Bell C, Zimmerle D, Bradley T, Olsen D, Young P. Scalable turbocharger performance maps for dynamic state-based engine models. International Journal of Engine Research. 2016; 17: 705-712.
14 Tu H, Chen H. Modeling of a compressor's performance map by fitting function methodology. Advanced Materials Research. 2013; 779-780: 1194-1198.
15 Don Arnold S. Electric boost compressor and turbine generator system. US patent nº: 7,958,727 B2, 2011.
16 Kaori-Heat exchanger manufacturer. Available from:http://www.kaori-bphe.com. Access data: 13 may 2018.

17 Begman TL, Lavine AS, Incropera FP, Dewitt DP. Fundamentals of heat and mass transfer. Seventh edition. Hoboken, USA: Wiley publications; 2011.
18 Trendewicz AA, Braun RJ. Techno-economic analysis of solid oxide fuel cell based combined heat and power systems for biogas utilization at wastewater treatment facilities. Journal of Power Sources. 2013; 233: 380-393.